ABSORPTION POWER CYCLE WITH LIBR SOLUTION WORKING FLUID – DESIGN OF THE PROOF-OF-CONCEPT UNIT

Václav Novotný[1,2]*, David J. Szucs[1,2], Jan Spale[1,2], Vaclav Vodicka[2], Jakub Mascuch[2], Michal Kolovratník[1]

[1]Czech Technical University in Prague, Faculty of Mechanical Engineering,
Technicka 4, Praha 6, 16607, Czech Republic
Vaclav.Novotny@cvut.cz

[2]Czech Technical University in Prague, University Centre for Energy Efficient Buildings,
Trinecka 1024, Bustehrad, 27343, Czech Republic

ABSTRACT

The most common technology for utilizing low temperature and low power heat sources in a decentralized power system is the organic Rankine cycle (ORC). Nevertheless, there are appearing new alternative concepts providing theoretically higher efficiency, but they are far behind the technological maturity level of the ORC. One such concept is an absorption power cycle (APC) working with an aqueous solution of lithium bromide (LiBr) as a working fluid.

According to our findings and theoretical studies, the perspective application of APC is in low power output of no more than a few dozens of kW, and for heat sources at temperatures below 150 °C. Other features of APC include a high temperature glide across heat exchangers resulting in high exergy efficiency, and large volumetric flow rate of the vapour allowing to build an efficient turbine for small power output.

To the best knowledge of the authors, this cycle has never been experimentally explored. To assess the possibilities of the actual application, a proof-of-concept APC unit is designed. This work is a methodological design analysis of an experimental unit based on a thermodynamic model presented. The design of the APC unit is adapted for the following heat source: heat input 20 kW from a topping ORC unit, in 90 °C water (intermediate cycle). Calculation and sizing model results in expected <0.5 kW turbine output with high and low pressures 13 kPa and 6 kPa respectively. Alongside with the calculation methodology, the final design of the APC unit is presented. The equipment consists of a custom shell & tube desorber (evaporator) and absorber (condenser) with a design described, an axial impulse turbine made by additive manufacturing from plastic and micro gear pumps. The construction of these components and of the whole apparatus is, at the time of writing this article, underway. Commissioning, experimental results, and a subsequent proof of application potential of the APC concept will be a subject of future work.

1. INTRODUCTION

Absorption principle is mostly known in refrigeration and cooling systems. Absorption cooling cycles represent the main category of thermally activated chillers. These cooling cycles have been already successfully used in their niche commercial applications recuperating low temperature heat, such as industrial waste heat to cover various cooling needs.

Absorption cycle can be also used for producing power; represented by e.g. Kalina cycle working with NH_3-H_2O mixture. Several studies have proven such cycle to be suitable and efficient for low temperature geothermal or waste heat recovery applications (Mirolli, 2012; Zhang, He and Zhang, 2012). Recently, a possibility of using LiBr solution, known from applications in the absorption chillers, has been suggested. Some works point out theoretical superiority of LiBr solution in efficiency to alternatives (Novotny and Kolovratnik, 2017), other pinpoint the suitability for low power applications due to the high volumetric flow rate of the vapour phase (suitable for turbines) or low system pressure reducing safety requirements (Novotny *et al.*, 2017).

However, no experimental works of these particular cycles with LiBr solution are known to the authors so far. Therefore, this work is among the first steps to the experimental verification of such cycle operation, as it shows a design of an APC proof of concept. Following the presented design, the unit is being built.

A general configuration of a general APC and a configuration of the experimental system being designed are shown in **Figure 1**. The unit will be part of an experimental cascade of cycles, so the heat source of the APC is a biomass-fired ORC where the heat is transferred by an intermediate water circuit. The working fluid in the desorber (steam generator in cooling cycle terminology) undergoes a partial phase change when steam is generated and goes through expander into the absorber. The rich solution is routed to absorber in a separate line via recuperator. While concepts with counter-flow low volume heat exchangers (as plate type) assume a separator downstream, our design follows a large volume exchanger design which already serves as a separator, as found in common absorption chillers. Note an additional pump in the rich solution line to overcome potentially excessive pressure losses in the line and nozzles in the absorber. In the absorber, the steam is absorbed into a subcooled liquid solution film flowing on a heat transfer surface where heat is removed into cooling water. In case of insufficient absorption rate additional solution recirculation circuit is considered here with the solution nozzles in the half of the absorber's height.

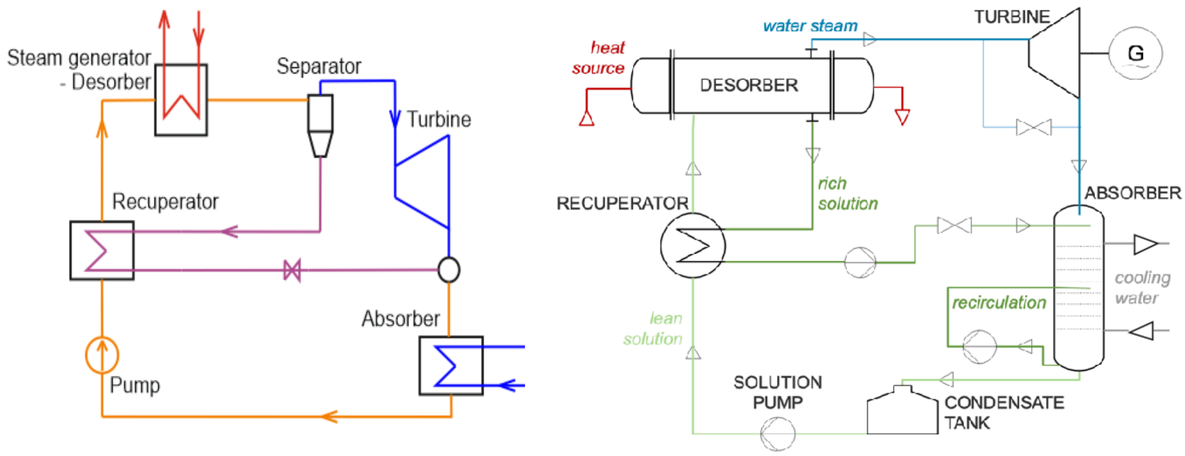

Figure 1: Schematic diagram of a general APC (left) and designed proof-of-concept APC unit (right)

2. EXPERIMENTAL UNIT

2.1 Performance requirements and boundary conditions

The main purpose of the designed APC unit is to serve as a proof of the whole concept as well as of specific components (e.g. 3D printed turboexpander). Therefore, the parameters were selected conservatively and rather similar to ones of absorption chillers, than according to theoretical results for the most efficient WHR system. It is expected, that the design would be later improved for increased efficiency, power output, reduction of components size and cost etc. The nominal condition is therefore selected as 20 kW_{th} of heat input with expected generator power output in hundreds of watts. The working pair and its mass concentrations were chosen according to the optimized values in the aforementioned publications. The summary of the main design parameters and expected performance is provided in **Table 1**.

Table 1: Main design parameters of the system

Heat source	Topping ORC with hot water circuit		
Inlet temperature of the heat source	T_{hs}	90	$°C$
Heat input	$\dot{Q}_{in}$	20	kW
Working pair	$H_2O - LiBr$		
Concentration of the lean solution	ξ_{lean}	35	% LiBr (mass)
Concentration of the rich solution	ξ_{rich}	50	% LiBr (mass)
Turbine design power output	$\dot{W}_{gross}$	0.3-0.5	kW
Heat sink	Cooling water closed circuit with dry cooler		
Inlet temperature of the cooling water	T_{rej}	30	$°C$

2.2 Theoretical model parameters

A theoretical model of the cycle has been described in detail in previous works as (Novotny and Kolovratnik, 2017) and is based on standard heat, mass and species conservation with heat transfer limited by the prescribed pinch points (12 K, 5 K and 10 K for desorber, recuperator and absorber respectively). Isentropic efficiency of the expander and pump has been preliminarily selected on the conservative values of 40 % and 20 % respectively. The thermodynamic model was created in Engineering Equation Solver (EES) based on the boundary conditions and assumptions stated. The thermodynamic properties of the working mixture were calculated using the LibWaLi library developed at Hochschule Zittau/Görlitz specifically for the lithium bromide – water mixture. (Kunick and Hasch, 2011) Main resulting parameters are given in **Table 2**.

Table 2: Main resulting parameters of the theoretical model

Total LiBr mass flow	$\dot{m}_{LiBr}$	0.0913	kg/s
Total water mass flow	$\dot{m}_{H_2O}$	0.0167	kg/s
High admission pressure	p_{HP}	13.38	kPa
Low emission pressure	p_{LP}	5.99	kPa
Heat source outlet temperature	$T_{hs,out}$	81.8	$°C$
Heat transferred in desorber	$\dot{Q}_{in}$	20	kW
Heat transferred in recuperator	$\dot{Q}_{rec}$	1.15	kW
Heat transferred in absorber	$\dot{Q}_{abs}$	19.63	kW
Turbine power output	$\dot{W}_{gross}$	0.37	kW
Required solution pump power	$\dot{W}_{pump}$	0.7	W
Required cooling water pump power	$\dot{W}_{cw;pump}$	42.1	W
Required cooling fan power	$\dot{W}_{fan}$	73.4	W
Net Plant power output	$\dot{W}_{net}$	0.26	kW
1st law efficiency of the cycle	$\eta_{1^{st}law;gross}$	1.9	%
Net 1st law efficiency of the plant	$\eta_{1^{st}law;net}$	1.3	%
Net exergy efficiency of the plant	$\eta_{ex;net}$	2.0	%

2.3 Design of components

The components of APC are rather specific and thus this section describes a chosen methodology and considerations foregoing the design. The construction of the device based on the chosen design is expected to be completed within the months to come.

2.3.1 Desorber and separator: Originally two conceptual configurations were considered. The first one was a plate heat exchanger with a vapour separator downstream and the second one was a single component heat exchanger of the shell & tube configuration (large volume, LiBr solution in the shell with specified liquid level), which is common to absorption chillers. Uncertainties linked to the actual operation of plate exchangers, the fact that the solution is only partly evaporated and an unknown regime of two-phase flow occurring in the heat exchanger causes the latter concept to be adapted for this experimental unit. In the calculations, it is still expected that the exchanger will behave in a counter-flow configuration with the goal to gradually increase the concentration of the solution and its temperature from the inlet to outlet. In order to approach this behaviour, a conceptual design of a single passage of both fluids in the exchanger is adopted.

For computational purposes, the exchanger has been discretized into 30 elements (each marked as i in the equations presented) of identical heat transfer. In each of these elements, the temperature difference between the heating water and the solution, variation in the properties of the fluid and the UA value are calculated. This way, the heat transfer coefficients are evaluated separately in each element as well. On the heating fluid side (water), Gnielinski correlation, presented in Equation (1), is used for the heat transfer coefficient evaluation.

$$Nu_{hs;i} = (f_{coef;i}/8) \cdot (Re_{hs;i} - 1000) \cdot \left[\frac{Pr_{hs;i}}{1 + 12{,}7 \cdot (f_{coef;i}/8)^{0,5} \cdot (Pr_{hs;i}^{0,67} - 1)}\right] \tag{1}$$

LiBr solution is in a saturated and nearly quiescent (very small velocity of flow) state along the entire exchanger. The boiling and evaporation take place at the submerged conditions, in the liquid solution. Pool boiling correlation shown in Equation (2) is adopted from (Charters *et al.*, 1982) to obtain the heat flux $\dot{q}_i$ iteratively with respect to the temperature difference between a hot wall surface and working fluid and then used to obtain the boiling heat transfer coefficient $\alpha_{boil;i}$. This equation is solved separately for each element. Conduction in pipes is included in overall heat resistance as well, although for simplicity of calculation, only as conduction through a flat plate (radial effects neglected).

$$\frac{c_{p,l,i}}{h_{fg,i}} \cdot (T_{surf,i} - T_i) = 0.0136 \cdot \left[\frac{q_i \cdot 10^{-3}}{\eta_{l,i} \cdot h_{fg,i}} \cdot \left[\frac{\sigma_{LiBr}}{g \cdot (\rho_{l,i} - \rho_{v,i})}\right]^{0.5}\right]^{0.34} \cdot \mathrm{Pr}_{l,i}^{0.85} \tag{2}$$

Following the described methodology, the resulting heat exchanger has a heat transfer surface area of 3,07 m^2, consisting of 70 tubes DN8 (13.5 x 2.35) with a functional length of 1.15 m. Temperature sensors along the shell length are incorporated to provide information on the actual temperature glide in this type of exchanger. The final design of the desorber is shown in **Figure 2a**.

2.3.2 Absorber: Experimental works have shown a large uncertainty in the absorption rate in comparison with the theoretical predictions. Furthermore, an absorber of the APC works at different conditions (higher emission pressure, higher temperatures and altered concentrations), than it is typical for the chiller cycle. For the efficient APC concept, a counter-flow absorber is required. Therefore, a rather simple methodology with subsequent oversizing and means of absorption improvements are adopted. The sizing is based on a convective mass transfer coefficient between the vapour and the liquid solution, as described in Equation (3), in which $\dot{m}_{H_2O}$ is vapour mass absorbed, k_l is mass transfer coefficient $[ms^{-1}]$, ρ_l is liquid density, Δc_{H_2O} is difference in concentration between saturated solution at given temperature and pressure and actual concentration of subcooled solution in the liquid film. The liquid film is here expected to be on all the heat transfer area *A*.

$$d\dot{m}_{H_2O} = k_l \rho_l \Delta c_{H_2O} dA \tag{3}$$

In order to ensure operation in the case of lower absorption rate, the surface area is oversized, and an additional recirculation of the solution is implemented. In order to keep as much as possible of the counterflow principle, to be able to assess the operation of this part as well as the performance extent of the recirculation, a second (lower) segment of the cooling coils is added underneath within the same absorber. Recirculation nozzles are placed into the middle of the entire absorber in between the two cooling coil segments of the same surface area. This modification multiplies the total surface area of the cooling coils needed by 1.9 in comparison to the theoretical model. Besides having covered an off-design operation, this enlargement of the area secures the uncertainty of the theoretical mass and heat transfer model.

The modelled absorber thus consists of two coil sections with parallel connection of cooling water. The section is designed with four DN15 (21.3 x 2.0) stainless pipes coiled at different diameters, each measuring about 20 metres in length. Temperature sensors are further added along the height to measure the temperature (bulk vapour, not film though). The resulting design is presented in **Figure 2b**.

2.3.3 Recuperator: There are no special requirements for the recuperator, which has liquid phase fluid on both sides. Thanks to a booster pump in the LiBr rich solution branch the pressure drop is not a major issue either. A flat plate exchanger is used, specifically, SWEP heat exchanger B5T with a size designed via manufacturer-provided sizing tool based on proprietary correlations

(a) (b)

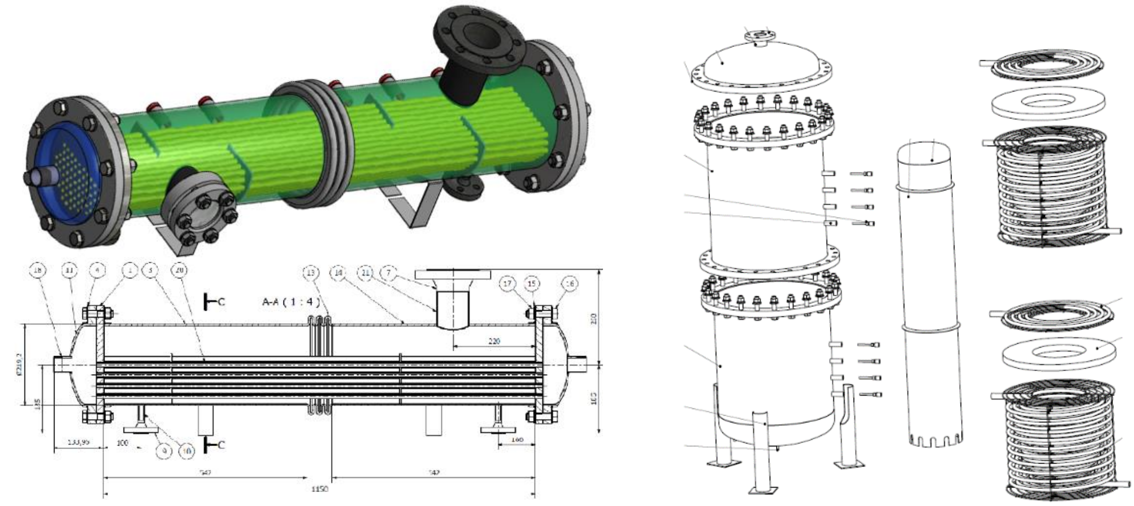

Figure 2: (a) Design of the desorber and (b) design of the absorber

2.3.4 Expander: Turboexpander concept is chosen due to the large vapour volumetric flowrates of the APC. Following suggestions of (Weiß, 2015), requirement of low cost components (lower speed, worse manufacturing tolerances etc.), an axial impulse turbine with partial admission has been designed for this application. The design is based on a 1D mean line model with chosen maximal rotational speed suitable for the generator and its bearings (only 15 000 rpm) and mean rotor diameter to ensure manufacturability with good tolerances (120 mm). Note that the turboexpander is manufactured by selective laser sintering (SLS) of polyamide powder and the design is the outcome of another project (Novotny *et al.*, 2018). The goal is to test this sintered turboexpander in operation at the APC unit. According to the design of the turbine model, the isentropic velocity is corrected by velocity coefficients which, together with correlations for other secondary losses (partial admission, secondary flow – horseshoe vortex loss, passage vortex loss, disc friction-ventilation loss and profile loss) and flow coefficients taken from (Ambroz, 1984). Nozzle angle and degree of partial admission are optimized in order to achieve maximal efficiency. With constraints in both rotating speed and diameter, the efficiency is away from the optimal values and its designed nominal value is 44 %. On the other hand, it is considered acceptable for a proof of concept unit with space for further improvement (only increase in speed could improve the efficiency over 70 %).

As the loading of the stages and operating temperatures are low, plastic material, which can be well 3D printed, is a sufficient material of nozzles and rotor buckets. The resulting concept is a turboexpander with stator nozzles ring and rotor buckets wheel manufactured in a single piece with the rotor directly mounted on a permanent magnet generator converted from aeromodelling BLDC motor. For simplicity, the design is then made in a way that the expander is inserted between flanges into the piping. The design is shown in **Figure 3**.

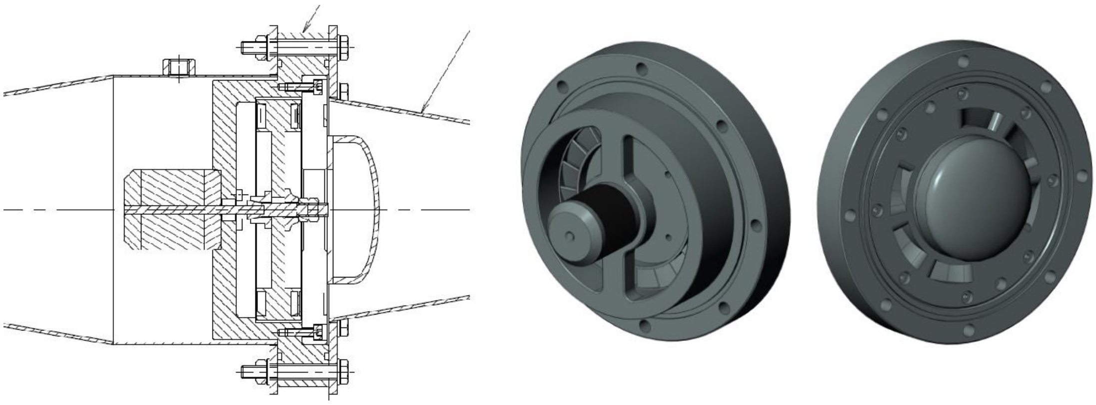

Figure 3: Design of the turboexpander

2.3.5 Solution pumps: Requirements for the pump are hermetic design, low required NPSH, corrosion resistance and very small volumetric flowrates in order of a few dozen ml s^{-1}. A micro gear pump driven via a magnetic coupling has been chosen as it seems to fulfil these requirements, particularly Topsflo MG213. The same micro gear pump is used as well for the booster pump on the rich solution and absorber recirculation pump.

2.3.6 Other: Due to the fact that the proposed apparatus is an experimental unit, it is equipped with additional components. These include pressure, temperature and volumetric flow measuring devices on all of the branches downstream and upstream the crucial components. As described before, thermometers are also installed within the desorber and absorber.

A solution tank is added downstream from the absorber, mainly to provide storage of the solution for both maintenance and operation with varying solution volumetric flow at different experimental regimes. The solution tank is equipped with an additional cooling coil in case of insufficient NPSH and a sight glass.

2.4 Whole system considerations

Besides having designed all the crucial components separately, thorough care needs to be taken regarding the interconnection of the whole system. The performance of the absorption process is heavily dependent on the interaction of the absorbent (lithium bromide solution) and the absorbate (water) in the components. In order to keep the low pressure needed in the whole system, a series of arrangements are taken into consideration. An air-tight quality welding is used in the manufacturing of components. In case of the interconnection of components, high-quality sealing (mostly Teflon or silicone based) is chosen on flanges on vapour side and NPT threads are used on other piping connections.

Another reason that raises the importance of a well-sealed system is the high risk of corrosion in case of oxygen intrusion. The water-LiBr solution is highly corrosive if it gets in contact with oxygen. For this reason, stainless steel is used as a material for all of the components. Although copper or carbon steel are common in absorption devices, it is not recommended for an experimental unit as oxygen intrusion and improper inhibitor choice might occur in higher frequency. Inhibitors that are added to the solution are lithium salts of chrome, molybdates and nitrates. During commissioning, the working space needs to be evacuated prior to charging the working fluid. For the same reason, during the long-term outages, nitrogen is introduced to protect the components from oxidation/corrosion processes.

3. RESULTS & DISCUSSION

The resulting main dimensions and parameters of the components are summarized in **Table 3**. Design of the overall system is then depicted in **Figure 4.** It is apparent that oversized experimental absorber, where maximal counter-flow temperature profile is intended, is by far the largest and the tallest of the components. A turbine is placed upstream, right above the absorber's inlet. The highest point is thus 4.3 m above the ground.

Design methods theoretically described in available literature mainly for desorber and absorber yield physically large components for this low-temperature heat source of 90°C. This is due to low operating pressures that accounts for large volumetric flows, small mass flow rates, and also due to the factor of design safety margin. Out of 20 kW of thermal heat input in the heating water, it is now 0.37 kW expected to be converted to power with the rest being rejected in the absorber. Net power respecting the own power consumption in the system is 0.26 kW. This yields a 1st law efficiency of the system of 1.3%. Although the system is thermodynamically partly optimized, this number might be either reduced due to further loses unforeseen or omitted in the calculation due to process and design uncertainties.

The power output of a few hundreds of watts is a result of a small pressure difference and low mass flow of the steam for the given heat input. These parameters, however, can be altered with a change in concentration difference. The design is performed for a constant concentration difference between lean and rich solution, but its impact on the cycle efficiency as well as the potential utilization efficiency of potential open loop (waste heat) heat source will be further explored. In absorption cooling, this concentration difference is largely limited due to specified evaporation pressure for chilling operation. Here, this parameter is not constrained, and theoretical results suggest high utilization efficiency for large concentration difference (and thus temperature glide). Operation with a large temperature glide, on the other hand, has not been reliably reported for absorption systems.

Table 3: Resulting parameters of the components

Component	Design	Dimensions	Performance
Desorber	Single pass Shell & Tube, LiBr in shell and heating water in tubes	70 pipes of DN8 (13.5 x 2.35) with a length of 1.15 m; liquid volume of 14.4 l	Heat load: 20 kW; min. $\Delta T = 12\ K$; $\dot{m}_{HS} = 0.58\ kg.s^{-1}$; $\dot{m}_{des,in} = 26.1\ g.s^{-1}$
Absorber	Spiral heat exchanger of two sections of cooling coils with distribution nozzles and packing; cooling water in tubes	4 spiral pipes of 20 m in length each in one coil section; section height: 0.86 m;	Heat rejection: 19.6 kW
Recuperator	Flat plate SWEP B5T	Specified by manufacturer	Heat load: 1.15 kW
Expander	3D printed (SLS, Polyamide PA 2200) axial single stage turbine with permanent magnet generator, design between flanges	D_{mean} = 120 mm, $D_{overall}$ = 230 mm	Nominal power 360 W, η_{is} = 44 % (15 000 rpm)
Pumps	Three identical pumps TOPSFLO MG213XK/DC24WI on lean solution feeding branch, on absorber recirculation and on rich solution branch	Specified by manufacturer	Flow scope: 300 – 3500 ml/s; power: 70 W

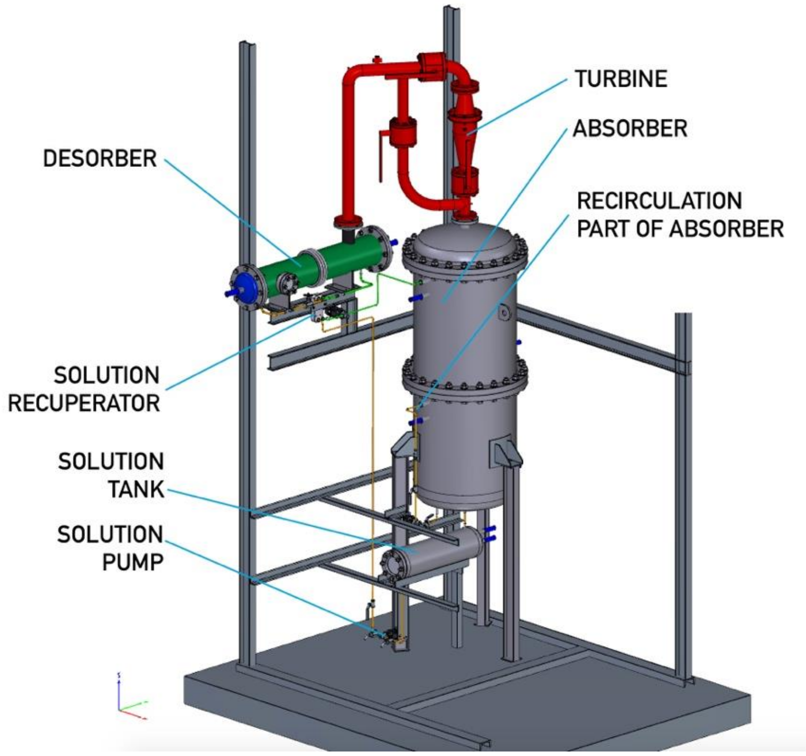

Figure 4: Overall design of the experimental APC unit (Red coloured components are for vapour branch, green for LiBr rich solution and light brown colour for LiBr lean solution)

3. CONCLUSION

A laboratory scale experimental absorption power cycle (APC) with LiBr solution has been designed. The system has nominal heat source temperature 90°C, heat input 20 kW and gross electrical output 370 W. Design is however made in order to have a working experimental system based on which possibilities for performance improvement will be investigated.

After the APC unit will have been successfully set up, to authors' best knowledge, it will be the first known APC operating with the lithium bromide solution. As there are large uncertainties in the design along with specific APC feature as very low pressures, the dimensions of the system are rather large. Operation and experimental results in future works will determine if and how the size can be reduced, design simplified, and performance improved in order to provide potentially competitive technology for the intended low temperature applications.

NOMENCLATURE

Symbols

A	Area	(m^2)
α	Convective heat transfer coefficient	(W m^{-2} K^{-1})
c	Concentration	(kg kg^{-})
c_p	Specific heat capacity	(J K^{-1} kg^{-1})
Δ	Difference	(1)
dm	Change in mass	(kg)
η	Dynamic viscosity	(Pa s)

η_{is}	Isentropic turbine efficiency	(%)
f_{coef}	Darcy friction factor	(1)
h_{fg}	Specific heat of vaporization	(kJ kg^{-1})
g	Gravitational acceleration	(m s^{-2})
k	Mass transfer coefficient	(m s^{-1})
m	Mass flow	(kg s^{-1})
Nu	Nusselt number	(1)
p	Pressure	(kPa)
Pr	Prandtl number	(1)
Q, q	Heat flow, heat flux	(kW, kW m^{-2})
Re	Reynolds number	(1)
ρ	Density	(kg m^{-3})
σ	Surface tension	(N m^{-1})
T	Temperature	(°C, K)
W	Power	(W, kW)
ξ	Mass concentration of LiBr	(kg$_{LiBr}$ kg$_{solution}^{-1}$)

Abbreviations

APC	Absorption power cycle
BLDC	Brushless direct current (motor)
DN	Nominal diameter
EES	Engineering Equation Solver
NPSH	Net positive suction head
SLS	Selective laser sintering
WHR	Waste heat recovery

Subscripts

1st law	With respect to 1st law of thermodynamics
abs	Absolute
boil	Boiling
gross	Gross
cw	Cooling water
ex	Exergy
fan	Fan
hs	Heat source
H_2O	Water

HP	High pressure
i	Element number
in	Inlet
l	Liquid
lean	Lean solution
LP	Low pressure
net	Net (power)
out	Outlet
rec	Recuperation
rej	Rejection
rich	Rich solution
surf	Surface
v	Vapour

REFERENCES

Ambroz, J. (1984) 'Parní turbíny a kondenzace (Steam turbines and condensation). Prague: CTU in Prague.

Charters, W. W. S. *et al.* (1982) 'Atmospheric and sub-atmospheric boiling of H2O and LiBr/H2O solutions', *International Journal of Refrigeration*, 5(2), pp. 107–114.

Kunick, M. and Hasch, S. (2011) 'Property Library for Mixtures of Water / Lithium Bromide FluidLAB with LibWaLi'.

Mirolli, D. (2012) 'Kalina cycle power systems in waste heat recovery applications', *Global Cement Magazine*.

Novotny, V. *et al.* (2017) 'Possibilities of water-lithium bromide absorption power cycles for low temperature, low power and combined power and cooling systems', *Energy Procedia*. Elsevier B.V., 129, pp. 818–825.

Novotny, V. *et al.* (2018) '3D Printing for Low-Cost Low-Parameters and Rapidly Developed Turboexpanders for Decentralized Micro-Power Systems', in *ASME Turboexpo 2018 (poster)*. Oslo.

Novotny, V. and Kolovratnik, M. (2017) 'Absorption power cycles for low-temperature heat sources using aqueous salt solutions as working fluids', *International Journal of Energy Research*, 41(7), pp. 952–975.

Weiß, A. P. (2015) 'Volumetric expander versus turbine – which is the better choice for small ORC plants', in *3rd ASME ORC Conference, Brussels (Belgium)*, pp. 1–10.

Zhang, X., He, M. and Zhang, Y. (2012) 'A review of research on the Kalina cycle', *Renewable and Sustainable Energy Reviews*. Elsevier, 16(7), pp. 5309–5318.

ACKNOWLEDGEMENT

This work was supported by the Grant Agency of the Czech Technical University in Prague, grant No. SGS OHK2-032/18, by project OPVVV mobility of junior researchers, no.: CZ.02.2.69/0.0/0.0/16_027/0008465, and by the Ministry of Education, Youth and Sports within National Sustainability Programme I (NPU I), project No. LO1605 - University Centre for Energy Efficient Buildings – Sustainability Phase and The Bavarian-Czech Academic Agency, grant no. BTHA-JC-2018-56, also 8E188012, Low cost turboexpanders for decentralized energy applications – possibilities of 3D print manufacturing from modern plastic materials.